Nano-Newton Force Spectroscopy of Silk

Biswajit Panda

A dissertation submitted for the partial fulfilment
of BS-MS dual degree in Science

Indian Institute of Science Education and Research Mohali
November 2016

Certificate of Examination

This is to certify that the dissertation titled **Nano-Newton Force Spectroscopy of Silk** submitted by **Mr. Biswajit Panda** (Reg. No. MS11051) for the partial fulfilment of **BS-MS dual degree programme** of the Institute, has been examined by the thesis committee duly appointed by the Institute. The committee finds the work done by the candidate satisfactory and recommends that the report be accepted.

Dr. Sanjeev Kumar Dr. Abhishek Chaudhari Dr. Kamal P. Singh
(Supervisor)

Dated: 30/11/2016

Declaration

The work presented in this dissertation has been carried out by me under the guidance and supervision of Dr. Kamal P. Singh at the Indian Institute of Science Education and Research Mohali.

This work has not been submitted in part or in full for a degree, a diploma, or a fellowship to any other university or institute. Whenever contributions of others are involved, every effort is made to indicate this clearly, with due acknowledgement of collaborative research and discussions. This thesis is a bonafide record of original work done by me and all sources listed within have been detailed in the bibliography.

Mohali, 30/11/2016

Biswajit Panda

In my capacity as the supervisor of the candidate's project work, I certify that the above statements by the candidate are true to the best of my knowledge.

Mohali, 30/11/2016

Dr. Kamal P. Singh

Acknowledgement

I would like to express my sincere gratitude to my supervisor, Dr. Kamal P. Singh, for his guidance, remark and encouragement throughout my masters thesis. Without his experience, this thesis wouldn't have been possible.

I would also like to thank my colleague Pooja Munjal for her endless assistance and motivation throughout my masters thesis. Also this thesis would not have been possible without the efforts of Dr. M. S. Siddhu, Gopal Verma, Komal Chaudhary and Gyanendra Yadav.

I would also like to acknowledge Shikha for encouraging me to explore science and being a source of inspiration. Ashish, Promit, Manaoj, Nitesh, Srikant, Aaveg, Anuj, Ruchika, Priyanka for helping me burn those midnight oil to finish this thesis.

Last but not the least, I dedicate this thesis to my parents, who believed in my talents and gave me the freedom explore my desire.

Biswajit Panda

Contents

List of Figures

Abstract

Spiders have been walking on the face of this earth for million of years, but very less is known about their silk construction to artificially recreate it. In this thesis, we explore this unexplored field. Using a new technique which can give us a force spectrum analysis of the response to stress, with the precision of 100 nN, we tried to understand the molecular deformation within the spider silk. Unlike many commercially available tensile testers, this new force spectroscopy is simple and versatile. In the scope of this thesis, we disclose various methods and techniques, like force relaxation method in which there is relaxation in the silk when subjected to a constant stress and multi-hysteresis cycle, through which one can get a detailed idea of the molecular deformation of spider silk to model the inside of it. We also explored the oscillation of the capture silk upon subjecting it to high voltage power supply.

Chapter 1

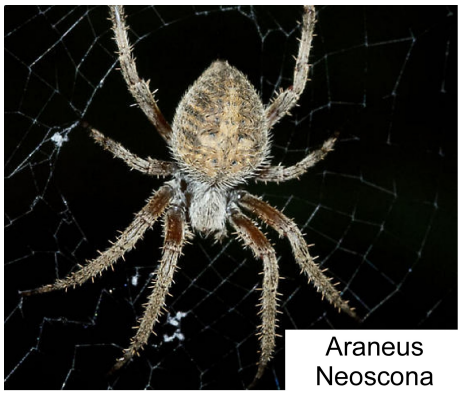

Araneus
Neoscona

Intoduction

An understanding of the natural world and what's in it is a source of not only a great curiosity but great fulfillment..

– David Attenborough.

Gone are the days, when naturally occurring polymers were the only source of creation of new materials. Today people are more focused on hybridizing the natural polymers with the existing technology to produce far better composites. These composites have improved the field of aviation, underwater exploration, space exploration, computers and many more, to help in providing a better understanding of the universe and also improve our lifestyles. One of the example of these modified composites will be *Silicones*, which is a silicon-based polymer. The bonding structure in this composites helps to bond with organic compounds to form polymers which are flexible and resistant to chemical attacks.

1.1 Spider

Spiders have been walking on the face of the Earth for millions of years. They have a very diverse group and can be found everywhere from deserts to tropical rain-forest to places with snow. Their sizes may vary from few millimeters to few centimeters. They are considered to be the most creative species. They catch their prey by building webs in thin air, which are rigid and elastic. These webs can absorb the kinetic energy of the flying or walking prey and once the prey is stuck to its web, its really hard for the prey to escape from it.

1.2 Spider Silk

The study of spiders is interesting because of its web, which is made of silks. These silks, not only serve the purpose of construction of web, but rather help spider in catching its prey, immobilizing it, provide a cushion for its egg and much more. To meet these uses, a spider actually produces different types of silks. The exact built of these spider silk are still unknown, which makes it more challenging. Given the need of production of better material for our day to day life, people have started exploring into spider silk.

1.2.1 Type of Silks

The glands in the abdomen of spider's are responsible in production of silk. Depending on the need, specific glands produces specific type of silk. The silk produces in the spider abdomen is initially in liquid state and then it is ejected out with high pressure that it converts into semi-solid state The various types of spider silks are as follows [5],

1. Major Ampullate (Dragline): This silk are considered to be the lifeline of a spider. Its used when spider senses a jerk and has to escape. Draglines are tough and elastic, so they do provide a outer rim to the web.

2. Minor Ampullate: Spiders use these silk as a temporary structure while the construction of actual web.

3. Flagelliform (Capture): This silk are unique in there own sense. These silk structure do contain glue beads, which helps for the prey to stick to the web. They constitute the major portion of the web. Apart from being sticky and highly elastic, these silk can extend to 300% of its natural length.

4. Tubuliform (Egg silk): This silk provides cushion for the eggs.

5. Aciniform: Once the prey sticks to the web, spiders use this silk to paralyze the prey, by wrapping it around the prey.

6. Piriform: These silk helps to stick different other silks in the construction of the thread.

1.2.2 What does spider silk look like?

In this section, we shall recall briefly the known structure of spider silk. S. Keten and M. Buehler have done extensive study by modeling what spider silk might look inside [1]. The model structure of spider silk is shown in Fig 1.1.

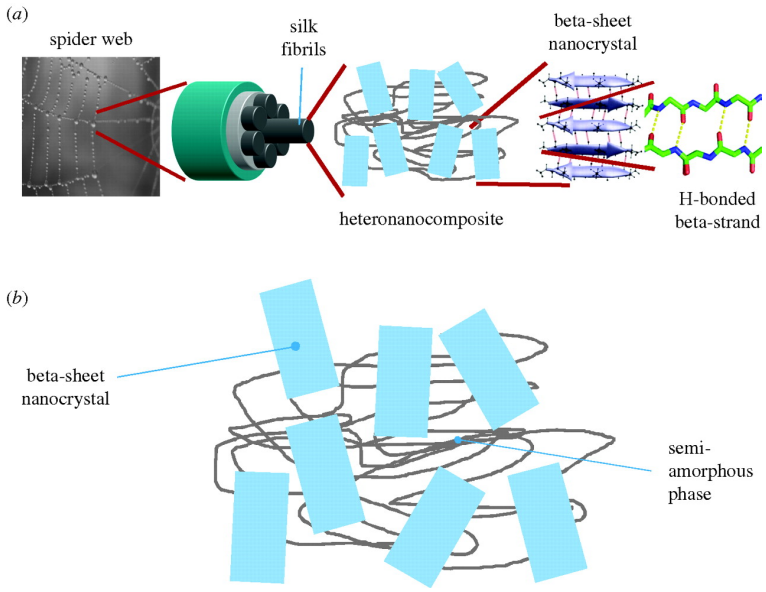

Figure 1.1: (a) Hierarchical structure of spider silk. (b) Beta-sheet nano-crystals are connected with each other through semi-amorphous protein chains, that are entangled [1].

Spider silk is composed of silk fibrils, which when zoomed in will have anti-parallel β-sheet crystals. These bunch of anti-parallel β-sheet crystals are connected with the other bunch through semi-amorphous chains, which are entangled among themselves, as shown in Fig 1.1. Within the bunch, these crystals are connected through H-bonding. Both β-sheet crystals and semi-amorphous chains play a very vital role in determining the strength, toughness and elasticity of the silk. The discussion of the exact structure of both these β-sheet crystals and semi-amorphous chains are beyond the scope of this thesis.

1.3 Stress-Strain curve for Dragline

In 1994, Y. Termonia [6] gave a brief theoretical understanding of the behavior of the spider silk. Based on that paper, J. Sirichaisit, R.J. Young and F. Vollrath [2] experimentally measured the stress-strain response for the spider silk with its Raman spectra at different stress to provide a

experimental proof to Termonia's theoretically calculated stress-strain curve.

r The stress-strain curve of any material is basic requirement to understand the material. This curve tells us the response of the material when it undergoes strain. The response is a result of the molecules rearrangement within the material when applied stress. A brief study of these dynamics can lead to an understanding of how the material is composed in the microscopic level. A detailled understanding of its inside structure is still unknown, so understanding of stress-strain response of the spider silk was necessary. In Fig 1.2, we can see the response of the single filament dragline silk of *N. edulis*. The stress-strain response was captured using Instron 1121 mechanical testing machine at strain rate of 0.01 min^{-1}. The diameter of the thread was in the range of 2-5 μm and the gauge length was 50 mm. The response is averaged over 10 fibers of same batch [2].

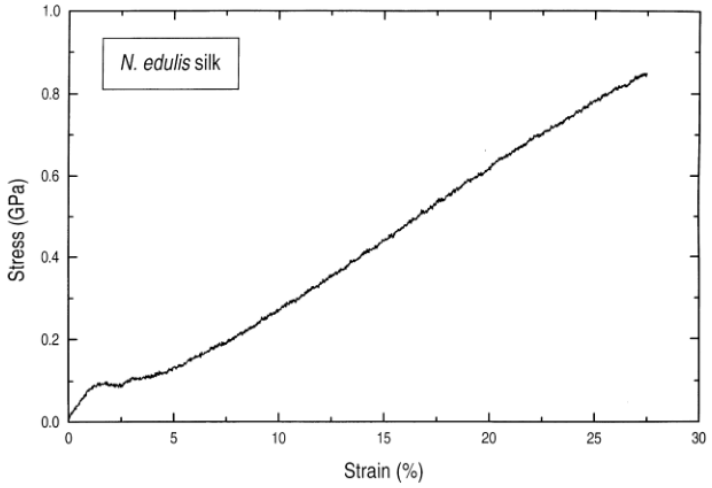

Figure 1.2: The stress-strain curve for *N. edulis* silk [2] .

If we zoomed into Fig 1.2 to a very small area, then we observe some noise in the graph. It is very hard to say whether this disturbance is actually noise from the machine or is it actual phenomenon happening within the dragline during the stress-strain experiment. Since there is some molecular rearrangement happening within the dragline, during the stress-strain experiment, if one improves the precision of the tensile tester then one can get a better understanding of the dynamics of dragline, like the bond breaking mechanisms, which can be used to further improve the microscopic picture of spider silk. In general, the precision range of commercially available tensile tester are in the range of mega-newton to micro-newton. We do have AFM's

which go till pico-newton, but they are not built to give us the stress-strain response that we are discussing in this section.

So can we device a setup to go to a scale to nano-newton (nN) precision, to measure the stress-strain response of any material?

Chapter 2

A versatile nano-Newton Force Spectroscopy

To know that we know what we know, and to know that we do not know what we do not know, that is true knowledge.

– Nicolaus Copernicus.

As discussed in Chapter 1, one needs to have a detailed understanding of the natural polymer to even think of making modified composites out of it. The very first step is to get a detail of the molecular arrangements in the natural polymers. The combined results from instruments like SEM, Raman and X-ray diffraction, can provide us with ideas of what is inside the material. Even a little information about the molecular arrangement could be drawn from the tensile study of the material. As discussed earlier, the stress-strain response, which is a result of the molecular level deformation, is studied by improving the precision of the tensile tester, we can experimentally observe the deformation.

With the currently commercially available tensile testers in the market, one can get a precision of micro-newton, with less room to modify or add new instrument to it. For example, one can add laser to the tensile tester, to simultaneously, get information about the surface deformation using diffraction technique along with the stress-strain response of the material. In the scope of this thesis, we will show a new technique that will be able to calculate the stress-strain response of any material in nN scale. This technique is simple and versatile, which allows us the room to add different instruments to take multiple readings simultaneously.

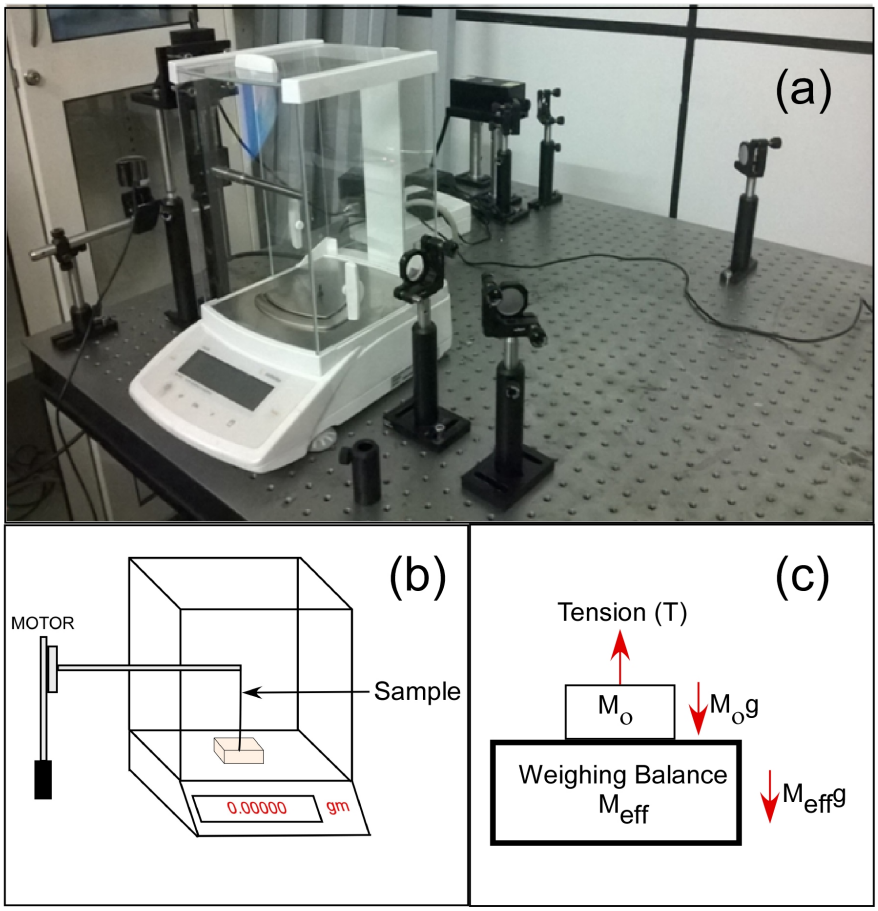

Figure 2.1: (a) Experimental Setup. (b) Schematic of the experimental setup, where one end of the sample is stick, using adhesive, to a mass kept on the micro-balance and the other to a support, which is screwed to the Thorlab motorized translational stage and (c) The force diagram for the setup.

This new force spectroscopy is just a combination of a micro/ultra-weighing balance with a motorized translational stage attached to it. For this thesis, we took Satarous micro-balance-CPA225D (maximum capacity = 100 gm, Readability = 0.01 mg, Repeatability = 0.05 mg, Linearity = 0.1 mg, Response time = 3 sec, Sensitivity Drift (10°C - 30°C) = $\pm$ 1 $ppm/°C$. We attached that to a Thorlab motorized translational stage (MTS50-Z8), which has a DC servo motor, travel range of 50 mm, with maximum velocity 4.5mm/s and maximum acceleration 2.4 mm/s^2. The motorized translational stage comes with an operating software Thorlab ATP Users, to control various parameters of the motor stage, like acceleration, velocity, displacement etc. The data from the micro-balance was captured in a computer using a third party software "Hyperterminal", which records the value of mass displayed on the micro-balance at

that instance. The data transfer is done using a RS232 cable, with 1200 bits/sec and average of 5 readings/sec. One end of the sample is cleaved to the the support that is screwed to the motorized stage and other to the mass kept on the micro-balance as shown in Fig 2.1(b).

2.1 Working Principle

The trick that makes this setup a force spectroscopy is the conversion of the mass into force. As shown in the Fig 2.1(c), when the motorized stage starts pulling up, there is a Tension ($T(t)$) induced in the sample. Thus the micro-balance will then show the effective mass (M_{eff}), given that the actual mass is M_o. The force equation then will be as follows,

$$T = (M_o - M_{eff}) \times g \tag{2.1}$$

Now, for a continuous change in the Tension (T) of the sample the equation can be rewritten as follows,

$$\Delta T = (M_o - \Delta M_{eff}) \times g \tag{2.2}$$

Using the above equation, one can calculate the precision and range of the Force Spectroscopy. Using the readability factor of the micro-balance, which is 0.01 mg, which is the least count of the micro-balance, and with the value of g as 10 m/s^2, the following can be derived,

$$\Delta T = (M_o - \Delta M_{eff}) \times g \tag{2.3}$$

$$\Rightarrow \Delta T = 0.01 \times 10^{-6} kg \times 10 m/s^2 \tag{2.4}$$

$$\Rightarrow \Delta T = 100 nN \tag{2.5}$$

Here the value of ΔT shows the change of the value of tension in the sample. With a precision of 100 nN, we can get a microscopic understanding of the sample when subjected to a stress.

From this section one can infer that, the precision of the setup can be improved by improving the readability factor of the micro balance. Now a days, micro balance with readability factor 0.1 μg are commercially available, which can, by using equation(2.3), give a precision of 1 nN.

2.2 Stability & Linearity

The weighing balances are made to measure the mass of a sample. One has to ensure that the value of mass remains constant or within an acceptable standard deviation, when measured for a long duration of time. The Fig 2.2(a) shows the stability of the mass for the micro-balance used for the proposed setup. The jump was in the range of $\pm$ 0.03 mg, equivalent to $\pm$ 300 nN.

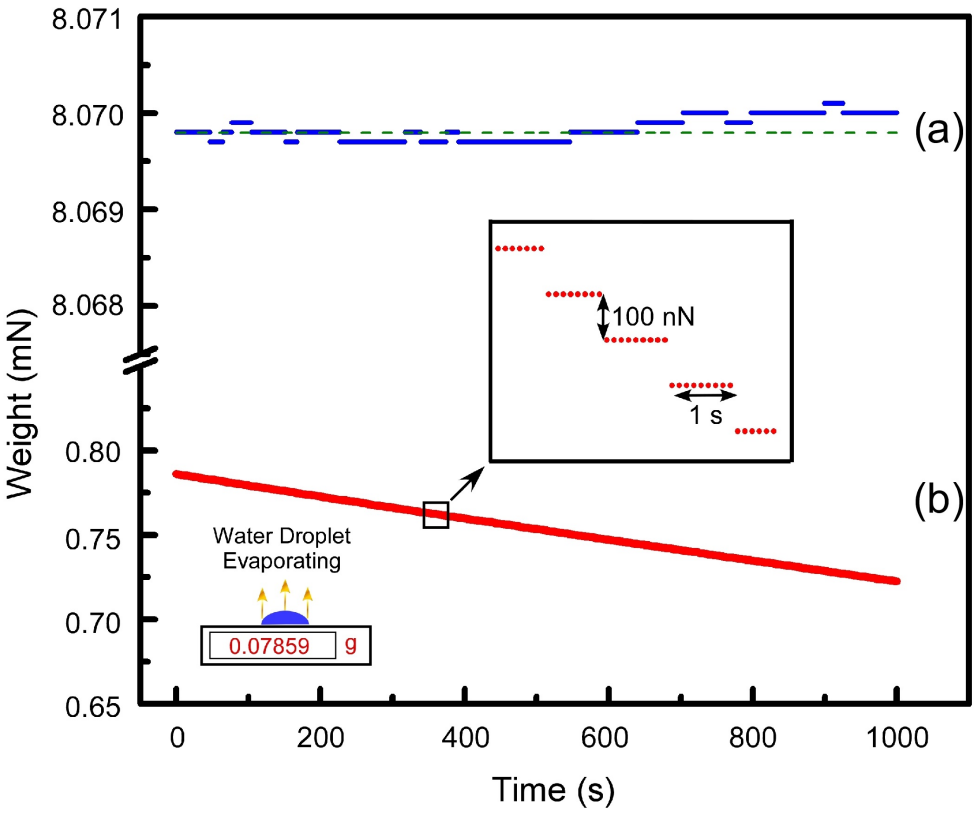

Figure 2.2: (a) The blue dots shows the value of a fixed mass when kept on the micro-balance, when kept for a long duration of time, and green solid dash line represents the rms value of the mass. (b) The water droplet evaporation as captured through the micro-balance. In the insert graph we have shown that since the rate of water evaporation is slower than the precision of the machine, so we gets steps of 100 nN, which is the machine precision. In the left lower side, schematic of water droplet evaporation setup is shown.

For a force spectroscopy, one is dealing with a continuous change in tension in a sample, so the proposed setup should be able to calculate and adapt to these continuous change. For this, calculating the rate of water droplet evaporation from our setup will do the job. The evaporation of a sessile water drop depends on the surrounding temperature and humidity .

The evaporation rate is very slow [7], way below the precision limit of the proposed setup. In principle, one should just observe a linear decrease in the graph with a jump step of the machine precision. Fig 2.2(b), shows a linear decrease in the weight of the water droplet. In the insert graph of Fig 2.2, one can see the jump of 100 nN, which is the precision limit of the machine. This establishes the fact, that proposed setup can handle a continuous change in the tension of a sample, when experimented with a stress.

2.3 Reference data reading

To finally claim that the proposed setup is a nono-newton force spectroscopy with stability in its reading and with a precision that can give a microscopic idea of sample's behavior, when subjected to stress, one has to reproduce pre-existing stress-strain curves of biological sample. The proposed force spectroscopy not only measures the stress-strain curve of any biological sample, but can also determine the change in the force within a sample due to its surroundings. In this section, one can see how versatile our proposed setup is.

2.3.1 Stress-Strain curve for Dragline using Force Spectroscopy

As mentioned earlier, the Dragline (Major Ampullate) is the most vital silk produced by the spider as it acts as a lifeline in case the spider senses any threat. We measured the stress strain response of *Araneus Neoscona* dragline silk using the new force spectroscopy.

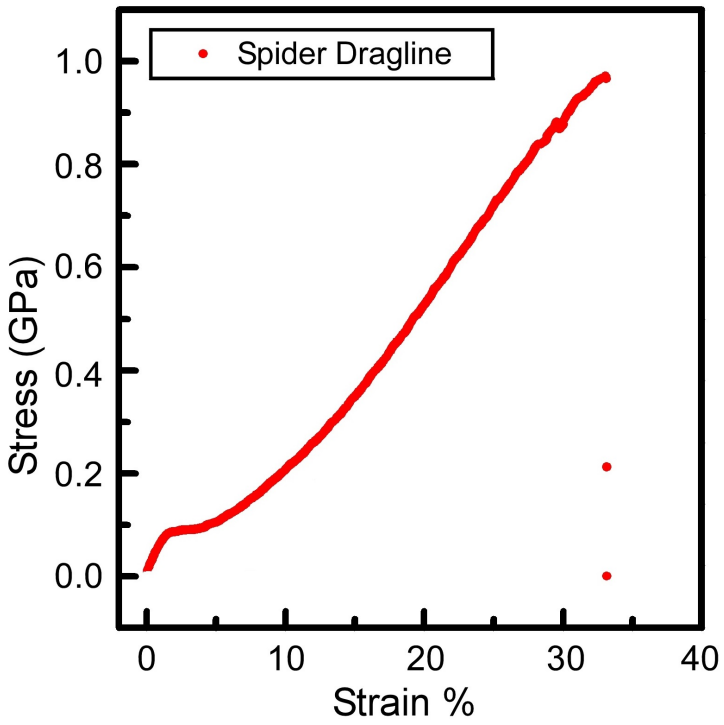

Figure 2.3: The stress-strain curve for *Araneus Neoscona* .

The setup was simple, where one end of the motor was cleaved to a slab placed on the micro-balance and other to the support that was screwed to the motor stage. The adhesive used was fevitite RAPID, and was allowed to dried for 1 hour so as it solidifies. The diameter of the thread was 2 μm, single filament, of length 68 mm. The motor stage was programed to operate at a strain rate of 0.02 min^{-1}.

The tensile strength and failure length for this particular setup was 0.96 GPa and 32%, which is similar to what was experimentally found by J. Sirichaisit, R.J. Young and F. Vollrath [2], as described in section 1.3. According to the Fig 2.3, there is a linearity after 5% of strain, which is believed to be because of the plastic behavior of the spider dragline. According to Y. Termonia [6], its believed that at this point, all the H-bonding within the bunch of anti-parallel β-sheet crystals breaks and there is deformation process proceeds to the semi-amorphous chains. Experimentally it has been found that, the crystals orientation improves, when the dragline is deformed, resulting in the reinforcement of the semi-amorphous chains, which leads to the silk elastic behavior [8].

2.3.2 Silk Cocoon as reference

Silk from the silkworm, which is the larva from the domesticated silk moth, Bombyx mori. Cocoon is made of a thread of raw silk. Silk Cocoon is not only a major raw material source for textile industries but also provides with medicinal properties, made it a valuable study for scientists for a long time.

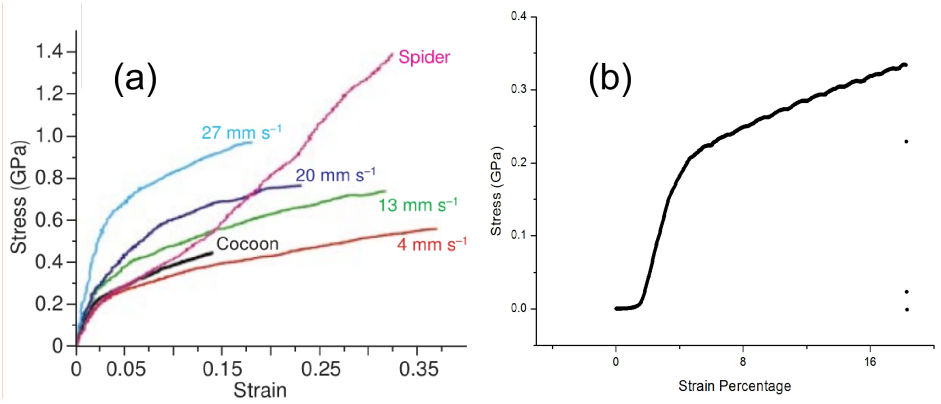

Figure 2.4: (a) Stress-strain curve of silk cocoon shown in the black solid line [3]. (b) Stress-strain curve of silk cocoon captured from the nN force spectroscopy.

In Fig 2.4(a), one can see stress-strain curve of silk cocoon proposed by Z. Shao and F. Vollrath [3] and in Fig 2.3(b), the same stress-strain curve of silk cocoon is shown, but taken from the new nano-newton force spectroscopy. The setup is similar as shown in Fig 2.1(b). The silk length was 87 mm with diameter 15 μm. The strain rate was programmed to 0.01 min^{-1}. Looking deep into Fig 2.3(b), then after 0.2 GPa stress, one can observe a particular jump pattern. Since the fact that the proposed force spectroscopy is stable and linear while taking a continuous change tension data, has been established in the earlier section, so the pattern in the Fig 2.4(b) is because of the sample. This pattern is absent in Fig 2.4(a), and the explanation for the pattern is beyond the scope of this thesis.

2.3.3 Leaf tearing and evaporation

As decribed in the start of this chapter that the proposed new force spectroscopy is unique as its simple and versatile simoultanously. These new spectroscopy can not only provide us data of deformation in only cyclindrical sized objects, which has been the case till now, but can

provide a good understanding of the deformation in any shape or size of sample.

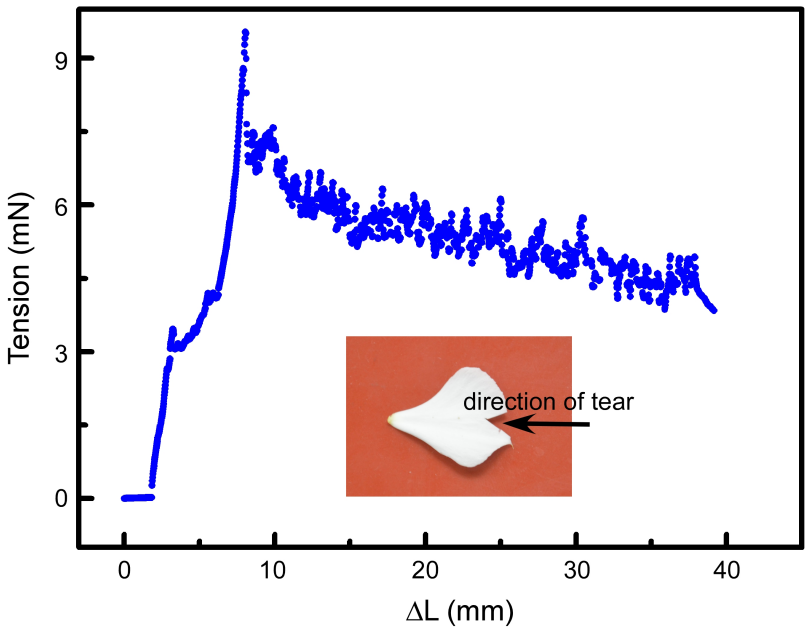

Figure 2.5: Force spectroscopy of flower tearing of the petal of Catharanthus roseus. It shows the rapture force of the flower with respect to the cut distance from the initial cut. The inner figure in the graph show the point where initial cut on the flower was done.

For this, a petal from Catharanthus roseus (Baramasi) was taken, a initial cut was placed on the flower as shown in Fig 2.5. One side along the cut was cleaved to the motor and the other to the slab placed on the micro-balance and then the motor was programmed to vertically go up at a strain rate of 0.01 min^{-1}.The adhesive used was fevitite RAPID, which was allowed to dried for 1 hour so as it solidifies. The whole setup could be imagined as tearing of a paper with both hands.As shown in Fig 2.5, the flower tearing graph. The thickness of the petal decreases as we go to the other end of the petal as shown in the Fig 2.5.

The whole setup could be imagined as tearing of a paper with both hands.As shown in Fig 2.5, the flower tearing graph. The thickness of the petal decreases as we go to the other end of the petal as shown in the Fig 2.5.It is beyond the scope of the thesis to explain the exact phenomenon going during the tearing effect. The decrease in the force while tearing might be because of the decrease in the thickness of the petal along the direction of the tear. Since the

proposed setup is linear and stable, so the fluctuation in the graph is a real phenomenon of the petal tearing, not because of the machine setup.

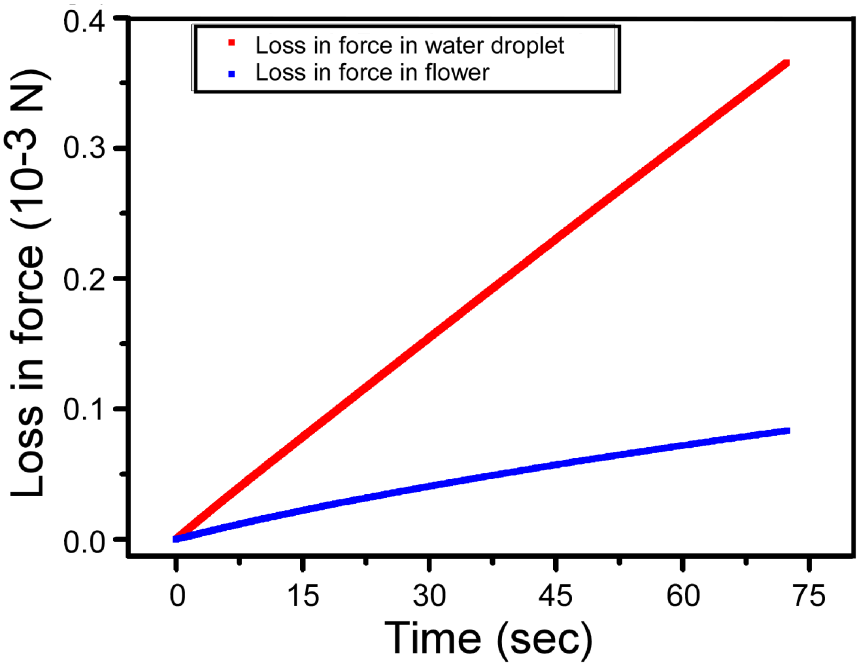

Figure 2.6: The read dot shows the loss in weight because of the evaporation of the water droplet kept on a slide. The blue dot shows the loss in the force because of the evaporation of water from a Catharanthus roseus petal, after it was plucked from the plant.

We know that the flower when plucked from a plant tends to dries off, the reason being that the water contained within these flowers evaporated. Fig 2.6 shows the loss in the force because of the evaporation of water from the Catharanthus roseus petal, after it was plucked from the plant. The loss of forces in both cases in Fig 2.6 are very slow process, beyond the setup's precision, so there were jumps of 100 nN, similar to that of Fig 2.2. The graphs in this section are meant to prove the versatility of the proposed setup. The explanation of the exact phenomenon in all these graphs is beyond the scope of this thesis.

Chapter 3

Experimental findings in Spider Silk

No matter what you're going through, there's a light at the end of the tunnel and it may seem hard to get to it but you can do it and just keep working towards it and you'll find the positive side of things..

– Demi Lovato.

3.1 Force Relaxation (FR) of Dragline

During the process of capturing the stress-strain for the using the nN force spectroscopy, if the motor was paused at any given strain, we did observe a force relaxation in the dragline. As mentioned in the previous chapter that due to the reinforcement of the semi-amorphous chain because the crystals become more organized due to deformation in the dragline, which result in the elastic behavior of the dragline. This can explain the force relaxation after the dragline was stressed to a fixed strain value.

To determine the force relaxation of *Araneus Neoscona* dragline, we took the similar setup as explained in section 2.2. The motor stage was programmed to go to desirable strain and then paused. The speed of the motor stage was programmed to 0.1 mm/s. Once the motor stage paused, the setup was left undisturbed. Since in this particular setup, there was no room for length expansion, so to balance out the stress induced in the dragline, there was relaxation in the tension. Fig 3.1 shows the force relaxation in *Araneus Neoscona* dragline at various strains.

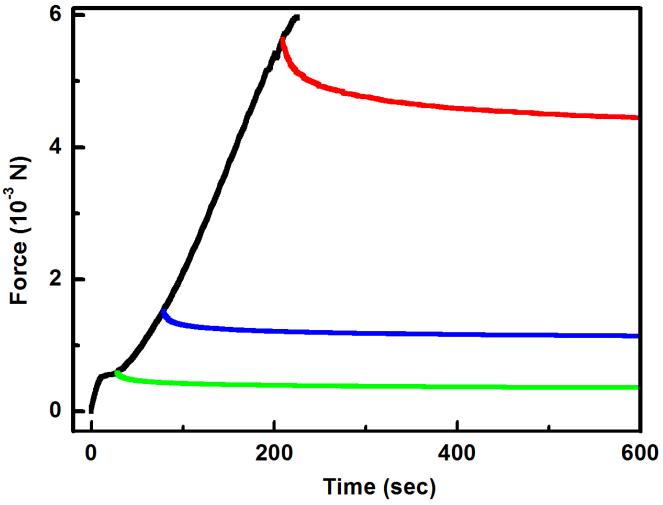

Figure 3.1: The force relaxation graph for *Araneus Neoscona* dragline. The black dots shows the stress-strain curve of the dragline. The green, blue and red dots are the force relaxation curve for 5%, 10% and 30% strains.

The behavior of dragline during force relaxation becomes clearer when Fig 3.1 is normalized.

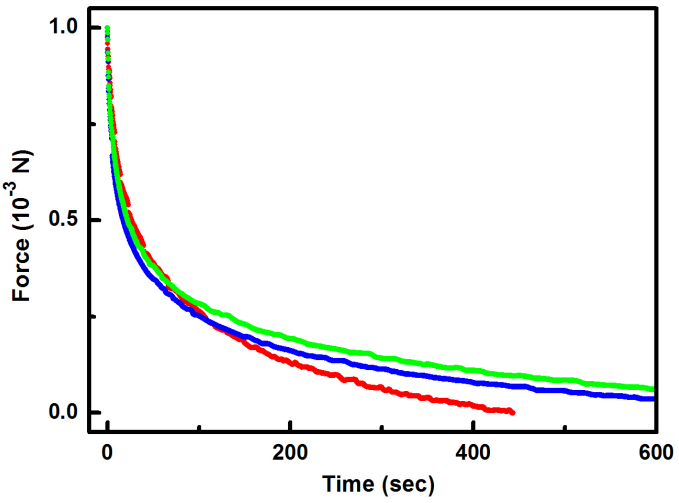

Figure 3.2: The force relaxation curves normalized. The green, blue and red dots are the force relaxation curve for 5%, 10% and 30% strains.

Hence it is clear from Fig 3.2, that the rate of force relaxation is higher in the case of higher strain percent.

It is obvious that during the force relaxation, there is a deformation of the bonding structure within the dragline. One way to know that is to plot the hysteresis graph before and after the force relaxation. Hysteresis tells us the energy dissipated due to the material internal working.

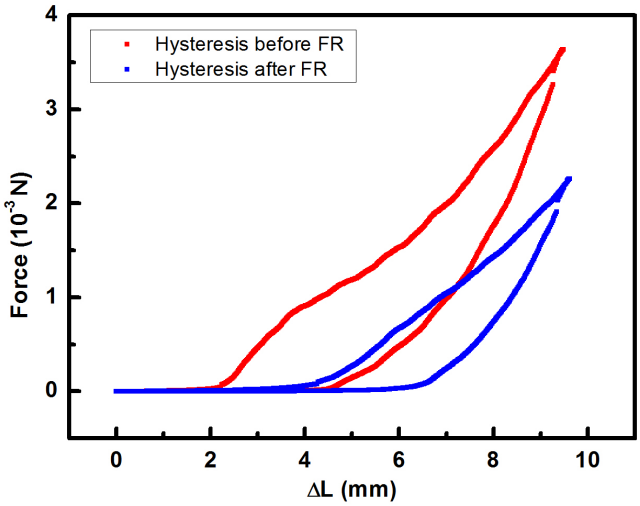

Figure 3.3: The hysteresis graph for *Araneus Neoscona* dragline. The red dot is the hysteresis curve for dragline without any strain and the blue dot is the hysteresis curve after force relaxation for strain 10%, with its exponential decay fit.

For measuring the hysteresis curve, we took the same setup as described in section 2.2. The motor stage was programmed to go till 10% strain in both the cases. The speed was set to 0.1 mm/s and acceleration/deceleration at 1 mm/s^2. First a freshly acquired dragline from *Araneus Neoscona* underwent through hysteresis, then another dragline from the same spider was first set to undergo force relaxation (10% strain) for half hour and then hysteresis process was done on it. Clearly from Fig 3.3, the area enclosed by the hysteresis curve is less after the force relaxation process, hence resulting to a less energy dissipation during the process of hysteresis. The only plausible explanation for this less energy dissipation for the hysteresis work, is that during the force relaxation process there is a damage in the bonding structure of the dragline and since there was no delay between the force relaxation and hysteresis (Fig 3.3 (blue)), so these bonds didn't get enough time to repair back.

3.2 Multi-cycle Hysteresis

As hysteresis gives us an idea of how much energy is spent if a sample is stressed from strain zero to strain ΔL and then back to strain zero. We calculated the graph for 30 hysteresis cycles for strain 10% of *Araneus Neoscona* dragline, which is shown in Fig 3.4. The strain rate was 0.02 min^{-1}.

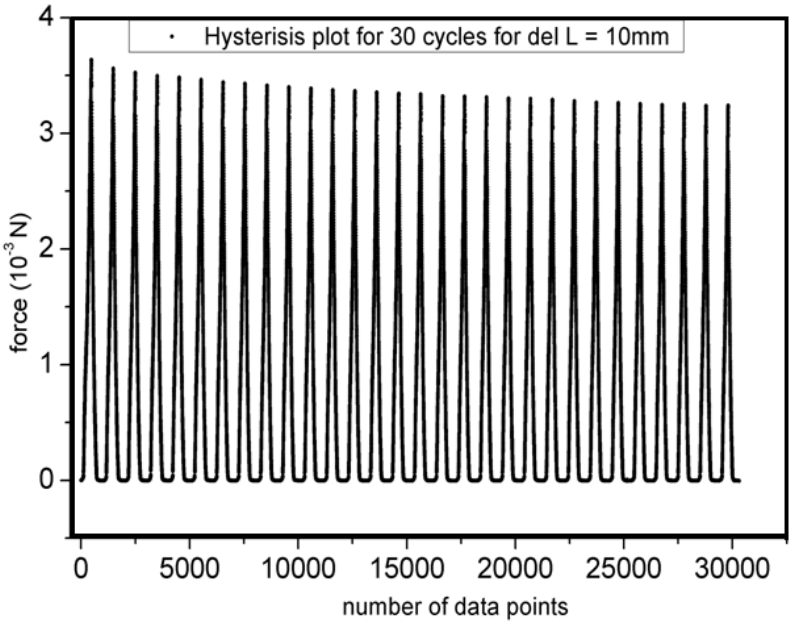

Figure 3.4: The 30 cycle hysteresis response for *Araneus Neoscona* dragline at strain 10%.

If one observes the Fig 3.4 carefully, there is a gradual decrease in the total force required for strain 10% over each hysteresis cycle. It is clear from the Fig 3.5, that the decrease in the amplitude for the maximum force per hysteresis has a best fit of an exponential decay. Spider dragline is consider to be highly tensile and elastic [9]. Because of its elastic nature, the molecular rearrangement or deformation should come back to its original configuration after certain elapse of time. If one can introduce another hysteresis cycle during this relaxation time, where the material is in process of regaining its original molecular conformation, then there will be a segment of the molecular conformation which would have not regain its original state.

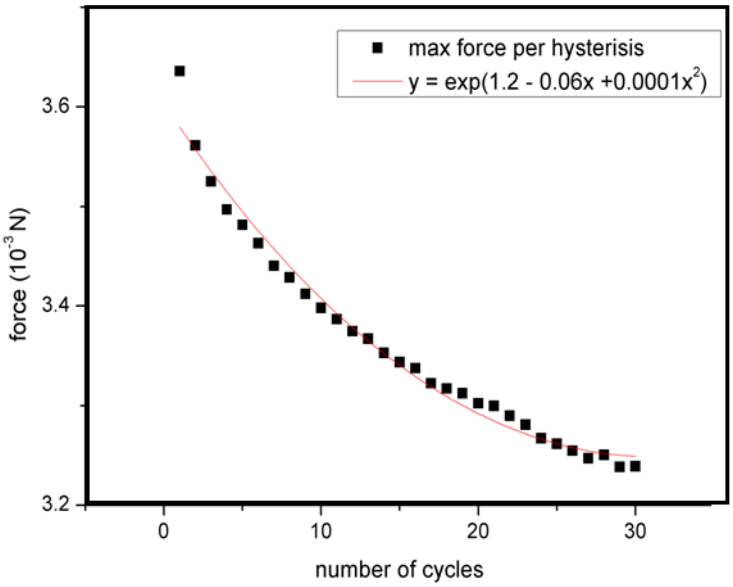

Figure 3.5: The decrease in the magnitude of stress for 30 cycle hysteresis for *Araneus Neoscona* dragline at strain 10 %.

Now this segment remains permanently deformed. So in the next hysteresis cycle, there will be no energy dissipated for that deformed molecular segment, hence the loss in the amplitude of stress for same strain percent, which is shown in Fig 3.5.

3.3 Miscellaneous Experiment on Spider Silk

3.3.1 Capillary action of oil in Dragline

The outer design of the dragline, as shown in Fig 3.6, is like two cylinders are stuck to each other, because of which there is a groove in it.

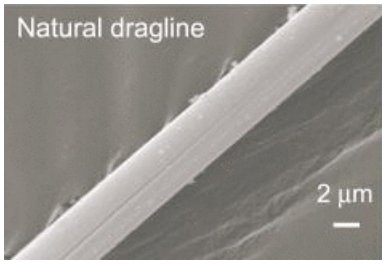

Figure 3.6: SEM image of *Araneus Neoscona* dragline silk.

When synthetic compressor oil (Sincom/32E, viscoity $40°C$: $27mm^2/s$, relative density $20°C$: $911kg/m^3$) was brushed on dragline using a very fine paint brush, then drops of oil was formed on it. With time, the number of drop decreased and the size of the drops remaining increased as shown in Fig 3.7. The whole phenomenon was recorded using a Thorlab CMOS Camera (DCC1645C) attached with a zoom lens. One of the possible explanation for this phenomenon might be because of the capillary action on the dragline because of the groove in the structure of the dragline.

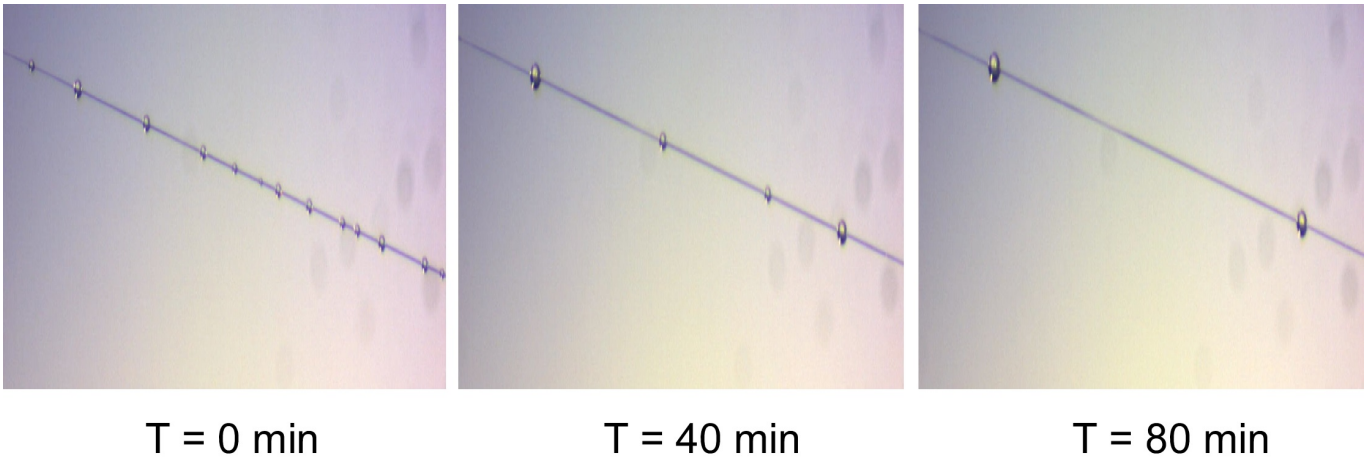

Figure 3.7: Synthetic compressor oil when brushed on *Araneus Neoscona* dragline silk. There was decreed in the number of the drops and increase in the size of the remaining drop for time zero minutes, 40 minutes and 80 minutes.

3.3.2 Capture Silk and Electrostatic effect on it

Spider web is consider to be nature's best architecture of trapping a pray. The web can absorb the all the kinetic energy of the prey, when it hits the web, and ensures that the prey is stuck to the web, giving time to the spider to reach it prey and paralyze it. All credit goes to Flagelliform silk or Capture silk, which are aligned in form of arcs joined to the radial thread. The ability of the capture silk to extend and contract along with the motifs placed on the silk thread, helps spider in its prey catching process. Capture silk has a tensile strength which is equivalent to that of steel, but its elastic strength surpass any made made material. It has ability to extend 300% of its natural length before braking, with its breaking energy per unit weight 20 times more than a high-tensile steel [10].

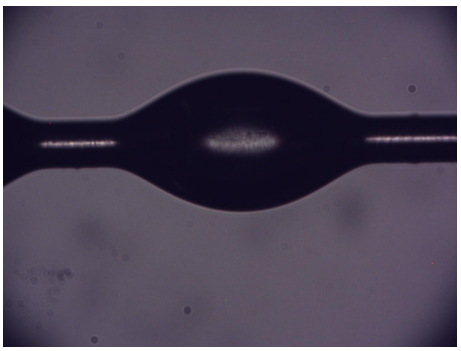

Figure 3.8: Zoomed image of capture silk from *Araneus Neoscona* orb web. The image was taken using Thorlab CMOS Camera (DCC1645C).

As one can see from Fig 3.8, the capture has these motifs, which are then organized into a hierarchy, forming structure modules on longer and longer length scale [11]. Apart from expressing these glue property, which helps to stick prey to the web, these motifs are a source of storing extra length of capture within, which helps it to elongate 300% of its natural length.

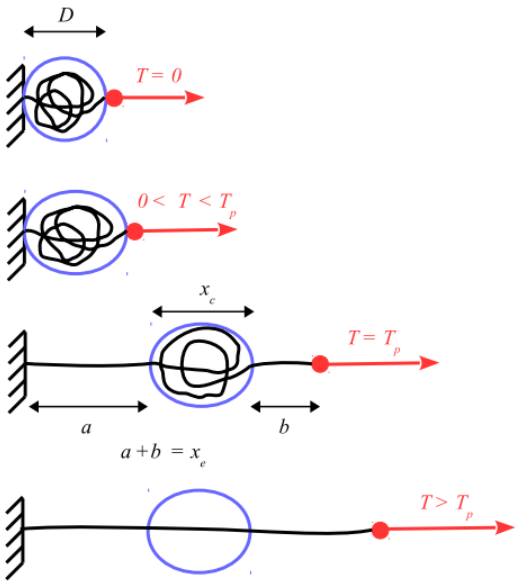

Figure 3.9: Extra length coiled inside the capture silk in each motifs. As the tension in the silk increases, the silk behaves like a spring till a certain tension T_p is achieved. T_p is the threshold tension till which the capture silk is like a spring. Once the tension threshold is crossed, the extra length in the motifs is contributes in the response of any further stress [4]

.

As shown by Vollrath and his team [4] in Fig 3.9, how a extra length of capture silk is actually coiled within these motifs, which actually provided these extra length for such an elongation of capture silk and how it is pulled out when it stress is applied to the capture silk. The surface tensions in these motifs are actually sufficient enough to let the extra length of capture silk coiled inside them.

But what happens when the length of the capture silk is compressed? The motifs which stores extra length of the capture silk, also coils in the natural length of the capture, when it is compressed. The whole process is called spooling action. During compression, all the motifs along the length of the capture silk also combines to provide a big space for more coiled length to be stored, as shown in Fig 3.10. Another particular property of the spider silk that can be deduced from Fig 3.10 is that the tension of the capture silk remains constant throughout the process of compression because of the spooling action.

Figure 3.10: Spooling action in *Araneus Neoscona* capture silk[ref]. At (I), the spring in this state behaves like a spring. At (II), the tension is decreased, the spooling action begins. At (III), almost whole length of capture is spooled inside a single motifs of capture silk [4].

Electrostatic effect on capture silk

In 1985, C. L. Craig and his team published a paper on the how spider web and insect oscillation correlates to the process of prey catching. In this paper, tehy described they model of how the oscillation of the spider web due to the air flow in the surroundings and the flight pattern of the insect, ultimately resulting in the collision of the insect to the web[12]. But recently, Robert Dudley and Victor Jimenez have experimentally shown that the spider web actually gets attracted towards the flying prey. Their paper describes the electrostatic charge acquired by the insects on their wings because of the free flight attracted the radial and spiral web[13].

Motivated by this, we took one single capture silk from *Araneus Neoscona* web kept it under

a microscope. The ends of the joints were attached to an insulator. A small metallic sphere connect to the positive terminal of a 10 KV DC power supply (PHYWE) where placed on the side of the silk without touching it. When increase in the voltage in the sphere, there was an increase in the oscillation of the capture silk was observed as shown in Fig 3.11.

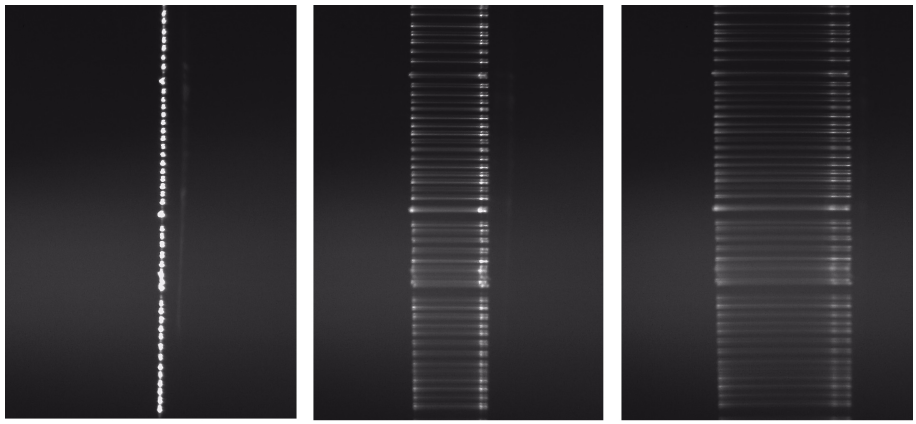

Figure 3.11: Oscillation of the capture silk at 1 KV, 3.5 KV and 5 KV.

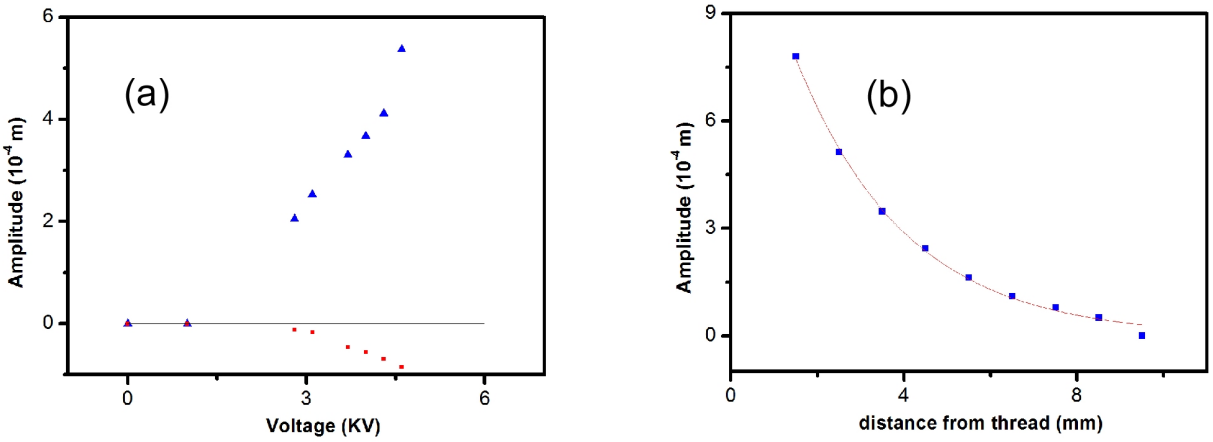

Figure 3.12: (a)Amplitude of oscillation of both sides along the equilibrium position of the capture silk with respect to voltage. The blue triangle shows the amplitude of the side where the charged metallic sphere was kept and the red square is showing the amplitude of the other side. The black line shows the equilibrium position of the capture silk. (b) Shows the variation of amplitude with respect to the distance of the charged sphere with a exponential decay best fit.

To the side where the charged sphere is kept the amplitude of is more compared to the other side. The change in the oscillation's amplitude of both sides with respect to the voltage is shown in Fig 3.12(a). The variation of amplitude with respect to the distance of the metallic charged sphere from the capture silk as shown in the Fig 3.12(b). The best fit shows an exponential decay of the amplitude with respect to the distance.

Chapter 4

Summary

To summarize the thesis, we started to tour with trying to explore in the area of spider silk. Their existence on the planet and their evolution have recently attracted lots of attention, because of the potential of spider silk and to artificially recreate it.n With missing detail of its internal structure, scientist are struggling their way to model one. In the first chapter, we started with understanding the stress-strain curve of spider silk dragline, which raised a question whether we can design a setup which can detect nN change in stress response of the dragline, thus leading a way to understand molecular level deformation within the spider silk while calculating its stress strain response.

In second chapter, we started with explaining why the requirement of nN force spectroscopy. Commercially made tensile tester provides a precision of micro-newton precision, thus we proposed a new nN spectroscopy, which is simple and versatile. We showed that the proposed new setup is stable to take readings for a long duration of time and can easily acquire readings for a stress-strain response of any material within a precision scale of 100 nN. With improving the micro balance, we can further go down the precision level to 1 nN. Unlike the commercially made tensile tester, this new setup provides a room of improvement so as to perform multiple experiment simultaneously.

In the third chapter, using the newly discussed force spectroscopy, we did various experiment on spider silk. To start with, we measured the force relaxation in dragline. When dragline is subjected to a constant stress in a constrain environment, then dragline changes its molecular orientation to relax its induced tension. This process if further explored in Raman spectroscopy, we can get the idea of these molecular reorientation, which can help us to model the spider silk.

Hysteresis tells us about the dissipated energy when work is done on the sample. Also due to the deformation of the molecular orientation due to the force/tension relaxation process, there will be less energy dissipated when same work is done on the dragline after the relaxation process. Also if one does multiple hysteresis cycle within the relaxation time of the dragline, this also induces permanent deformation in the molecular structure of the spider dragline, which was reflected in the hysteresis curve. These methods to understand the change in the molecular deformation can bring us closer to the understand the molecular building within the dragline.

Also the surface morphology in the dragline is such that it has a groove in it. This groove can result in capillary action on the surface of the spider dragline. The synthetic compression oil, which has surface tension enough to actually led to the capillary action on the surface of the dragline. There was decrease in the number of oil droplet with the diameter of the remaining droplets increasing, with time, is definite proof that the capillary action on the surface of the spider dragline.

Capture silk is most amazing natural fibre that exist in this world. With the ability to glue the prey to it, while absorbing all the kinetic energy transferred to it when it struck to it, is simply phenomenal. Less was actually know about the interaction of the capture silk and prey upon intersection, until recently it was found that there is a static charge involvement in the whole process. Studies have shown that during the random path flight of the insect, there is a static charge built up on the wings of the insect. These static charge on the wing actually pulls the radial and spiral thread of the web, towards it. Motivated from this, we tried to study the interaction of single capture thread due to the static charge. A small charged sphere, when introduced to the capture silk, it started to oscillated, with more amplitude towards the sphere. The amplitude varied with the voltage and distance of the sphere and capture silk.

In the future we would like to continue exploring these results in greater details. We shall also develop simple physical models to account for our experimental results.

Bibliography

[1] Sinan Keten and Markus J Buehler. Nanostructure and molecular mechanics of spider dragline silk protein assemblies. *Journal of the Royal Society Interface*, 7(53):1709–1721, 2010.

[2] J Sirichaisit, RJ Young, and F Vollrath. Molecular deformation in spider dragline silk subjected to stress. *Polymer*, 41(3):1223–1227, 2000.

[3] Zhengzhong Shao and Fritz Vollrath. Materials: Surprising strength of silkworm silk. *Nature*, 418(6899):741–741, 2002.

[4] Hervé Elettro, Sébastien Neukirch, Fritz Vollrath, and Arnaud Antkowiak. In-drop capillary spooling of spider capture thread inspires highly extensible fibres. *arXiv preprint arXiv:1501.00962*, 2015.

[5] Aimee Cunningham. Taken for a spin: Scientists look to spiders for the goods on silk. *Science News*, 171(15):231–234, 2007.

[6] Yves Termonia. Molecular modeling of spider silk elasticity. *Macromolecules*, 27(25):7378–7381, 1994.

[7] Gopal Verma and Kamal P Singh. Time-resolved interference unveils nanoscale surface dynamics in evaporating sessile droplet. *Applied Physics Letters*, 104(24):244106, 2014.

[8] David T Grubb and Lynn W Jelinski. Fiber morphology of spider silk: the effects of tensile deformation. *Macromolecules*, 30(10):2860–2867, 1997.

[9] Bhupesh Kumar, Ashish Thakur, Biswajit Panda, and Kamal P Singh. Optically probing torsional superelasticity in spider silks. *Applied Physics Letters*, 103(20):201910, 2013.

[10] JM Gosline, PA Guerette, CS Ortlepp, and KN Savage. The mechanical design of spider silks: from fibroin sequence to mechanical function. *Journal of Experimental Biology*, 202(23):3295–3303, 1999.

[11] Haijun Zhou and Yang Zhang. Hierarchical chain model of spider capture silk elasticity. *Physical review letters*, 94(2):028104, 2005.

[12] Catherine L Craig, Akira Okubo, and Viggo Andreasen. Effect of spider orb-web and insect oscillations on prey interception. *Journal of theoretical biology*, 115(2):201–211, 1985.

[13] Victor Manuel Ortega-Jimenez and Robert Dudley. Spiderweb deformation induced by electrostatically charged insects. *Scientific reports*, 3, 2013.

[14] Hervé Elettro, Sébastien Neukirch, Fritz Vollrath, and Arnaud Antkowiak. In-drop capillary spooling of spider capture thread inspires hybrid fibers with mixed solid–liquid mechanical properties. *Proceedings of the National Academy of Sciences*, page 201602451, 2016.

[15] Fritz Vollrath. Biology of spider silk. *International Journal of Biological Macromolecules*, 24(2):81–88, 1999.

[16] Andrea Nova, Sinan Keten, Nicola M Pugno, Alberto Redaelli, and Markus J Buehler. Molecular and nanostructural mechanisms of deformation, strength and toughness of spider silk fibrils. *Nano letters*, 10(7):2626–2634, 2010.

[17] Fritz Vollrath. Strength and structure of spiders silks. *Reviews in Molecular Biotechnology*, 74(2):67–83, 2000.

[18] Federico Bosia, Markus J Buehler, and Nicola M Pugno. Hierarchical simulations for the design of supertough nanofibers inspired by spider silk. *Physical Review E*, 82(5):056103, 2010.

[19] JD Van Beek, S Hess, F Vollrath, and BH Meier. The molecular structure of spider dragline silk: folding and orientation of the protein backbone. *Proceedings of the National Academy of Sciences*, 99(16):10266–10271, 2002.

[20] Fritz Vollrath, Thor Holtet, Hans C Thogersen, and Sebastian Frische. Structural organization of spider silk. *Proceedings of the Royal Society of London B: Biological Sciences*, 263(1367):147–151, 1996.

[21] Sinan Keten and Markus J Buehler. Atomistic model of the spider silk nanostructure. *Applied physics letters*, 96(15):153701, 2010.

[22] Cheryl Y Hayashi, Nichola H Shipley, and Randolph V Lewis. Hypotheses that correlate the sequence, structure, and mechanical properties of spider silk proteins. *International Journal of Biological Macromolecules*, 24(2):271–275, 1999.

[23] Markus J Buehler, Sinan Keten, and Theodor Ackbarow. Theoretical and computational hierarchical nanomechanics of protein materials: Deformation and fracture. *Progress in Materials Science*, 53(8):1101–1241, 2008.

[24] Steven W Cranford, Anna Tarakanova, Nicola M Pugno, and Markus J Buehler. Nonlinear material behaviour of spider silk yields robust webs. *Nature*, 482(7383):72–76, 2012.

[25] Yi Liu, Zhengzhong Shao, and Fritz Vollrath. Relationships between supercontraction and mechanical properties of spider silk. *Nature materials*, 4(12):901–905, 2005.

[26] Nathan Becker, Emin Oroudjev, Stephanie Mutz, Jason P Cleveland, Paul K Hansma, Cheryl Y Hayashi, Dmitrii E Makarov, and Helen G Hansma. Molecular nanosprings in spider capture-silk threads. *Nature materials*, 2(4):278–283, 2003.

[27] John M Gosline, M Edwin DeMont, and Mark W Denny. The structure and properties of spider silk. *Endeavour*, 10(1):37–43, 1986.